

New *N*(4)-methylthiosemicarbazone derivatives: Synthesis, characterization, structural properties, DNA interactions and antiproliferative activity

Mouayed Hussein ^{1,2,*} and Teoh Siang Guan ²

¹ Department of Chemistry, College of Science, University of Basrah, Basrah, 61001, Iraq

² School of Chemical Science, Universiti Sains Malaysia, Minden, Pulau Pinang, 11800, Malaysia

* Corresponding author at: Department of Chemistry, College of Science, University of Basrah, Basrah, 61001, Iraq.
 Tel.: +964.40.7800196370. Fax: +964.40.7800196370. E-mail address: mouayed_505emar@yahoo.com (M. Hussein).

ARTICLE INFORMATION



DOI: 10.5155/eurjchem.6.4.451-460.1318

Received: 11 September 2015

Received in revised form: 01 October 2015

Accepted: 10 October 2015

Published online: 31 December 2015

Printed: 31 December 2015

KEYWORDS

DNA binding
 Electronic transitions
 X-ray crystal structure
 Fluorescence emissions
 Antiproliferative activity
N(4)-Methylthiosemicarbazone

ABSTRACT

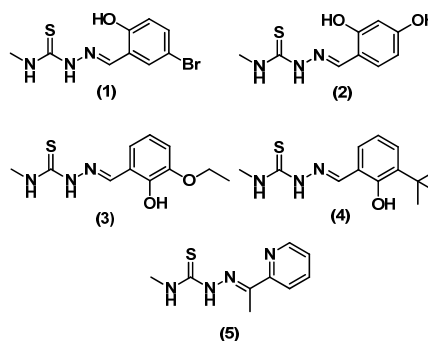
Five new thiosemicarbazone compounds derived from *N*(4)-methylthiosemicarbazide and 5-bromo-2-hydroxybenzaldehyde (1), 2,4-dihydroxybenzaldehyde (2), 3-ethoxy-2-hydroxybenzaldehyde (3), 3-*tert*-butyl-2-hydroxybenzaldehyde (4), and 2-acetylpyridine (5) have been synthesized. The molecular structures of the prepared compounds were identified using by single crystal X-ray crystallography. The binding properties of the compounds with *cal*/*thymus* DNA were analyzed by UV, fluorescence titration, and viscosity measurements. The cytotoxic properties of the compounds were tested against human colorectal cell lines (HCT 116). The compounds showed greater pronounced activity than the standard reference drug 5-fluorouracil (IC₅₀ = 7.3 μM). The results showed that the activity strength of these compounds depends on the lipophilic properties that provided by the terminal *N*(4)-substituent and aromatic ring-substituent, as well as the planarity that provided by the geometrical and conformational structures of the compounds.

Cite this: *Eur. J. Chem.* 2015, 6(4), 451-460

1. Introduction

The discovery of the antiviral, antibacterial and antitumor activities of the thiosemicarbazone ligands has stimulated numerous investigation concerning synthesis, characterization and biological relevance of such compounds [1-6]. Thiosemicarbazones belong to a large group of thiourea derivatives, whose biological activities are a function of parent aldehyde or ketone moiety [7,8]. Conjugated N-N-S tridentate ligand system of thiosemicarbazide seems essential for anticancer activity, possibly due to the observation that structural alterations that hinder a thiosemicarbazone's ability to function as a chelating agent tend to destroy or reduce its medicinal activity [9]. Furthermore, structural studies have shown that thiosemicarbazone derivatives containing phenolic oxygen have very interesting complexing properties, acting as tridentate O-N-S donor ligands [10-15]. The molecular interaction of compounds and DNA has received increasing interest in recent years because of its importance in design and development of chemotherapeutic drugs, this interaction is important for understanding the molecular mechanism of drug action for designing a specific DNA targeted drug [16-20]. From the other hand, the antiproliferative activity of compounds also has received more attention because such

compounds can be used as agents in biotechnology for development a new drugs [21-23]. Recent studies showed that the substitution on the terminal *N*(4) of thiosemicarbazone is much improved their biological activities [24-27]. We here report the synthesis, characterization, structural elucidation, DNA binding and antiproliferative activity for novel derivatives of *N*(4)-methylthiosemicarbazones shown in Scheme 1.



Scheme 1

2. Experimental

2.1. Materials and instrumentation

Melting points were measured using a Stuart Scientific SMP1 melting point apparatus. The infrared (IR) spectra were recorded on a Perkin Elmer system 2000 spectrophotometer using the KBr disc method. The ^1H and ^{13}C NMR spectra were recorded on a Bruker 500 MHz, using tetramethylsilane as an internal standard and $\text{DMSO-}d_6$ as the solvent. Elemental analysis was carried out using a Perkin Elmer 2400 series-11 CHN analyzer. The electronic and fluorescent spectra were recorded on a Perkin Elmer Lambda-35 spectrophotometer and a Jasco FP-750 spectrophotometer, respectively. X-ray crystallographic data were recorded on a Bruker SMART CCD diffractometer using graphite monochromated $\text{MoK}\alpha$ radiation ($\lambda = 0.71073 \text{ \AA}$) at 100 K. The data collected were reduced using SAINT program. The structure of all compounds was solved using the SHELXL-97 software package, and the molecular graphics were created using SHELXTL [28]. All non-hydrogen atoms were anisotropically refined. All of the chemicals, including thiosemicarbazide, aldehydes, and the solvents were purchased from Sigma-Aldrich.

2.2. DNA binding assay

The binding of compounds with *calftymus* DNA (CT-DNA) were investigated in 6.3 mM Tris-HCl/50 mM NaCl buffer (pH = 7). The DNA stock solution was prepared by dissolving a suitable amount of DNA in 6.3 mM Tris-HCl/50 mM NaCl buffer (pH = 7) at room temperature and stored in refrigerator for 2 days. A solution of CT-DNA in the buffer provided a UV absorbance ratio at 260 and 280 nm of ca. 1.9:1, which indicates that the DNA was sufficiently free of protein. The DNA concentration was estimated by the UV absorbance at 260 nm using the known molar absorption coefficient of $6600 \text{ M}^{-1}\text{cm}^{-1}$ [29]. The UV-Vis spectra were scanned at wavelengths ranging from 230 to 600 nm using the Tris/HCl buffer solution as the reference. Fluorescence emission assay was carried out using the aforementioned method. Fluorescence spectra were scanned at wavelengths ranging from 200 to 800 nm using the Tris/HCl buffer solution as the reference. Viscosity was measured using a Cannon Manning Semi-Micro viscometer immersed in a thermostatic water bath at 37 °C. Flow times were measured manually with a digital stopwatch. Viscosity values were calculated from the observed flow time of DNA-containing solutions (t) corrected by observed flow time of solvent mixture used (t_0), $\eta = t - t_0$. Viscosity data are presented as $(\eta/\eta_0)^{1/3}$ versus the ratio of the concentration (r) of the ligand-DNA solutions, where η and η_0 are the viscosity of the ligand in presence of DNA and the viscosity of DNA alone, respectively [30].

2.3. Antiproliferation assay

2.3.1. Preparation of cell culture

Human colorectal cancer cells (HCT 116) were grown under optimal incubator conditions. Cells that have reached a confluency of 70-80% were chosen for cell plating purposes. Old medium was replaced by aspiration. After that the cells were washed with sterile phosphate buffered saline (PBS) (pH = 7.4), 2-3 times, the intact layer of attached cells was subjected to trypsinization. Cells were incubated at 37 °C in 5% CO_2 for 3-5 min. Then, the flasks containing the cells were gently tapped to aid cells segregation and observed under inverted microscope (to confirm the segregation of the cells is completed). Trypsin activity was inhibited by adding 5 mL of fresh complete media supplied with 10% fetal bovine serum (FBS). Cells were counted and diluted to get a final concentration of 2.5×10^5 cells/mL, and inoculated into wells

(100 μL /well). Finally, plates containing the cells were incubated at 37 °C with an internal atmosphere of 5% CO_2 .

2.3.2. MTT assay

Cytotoxicity of the compounds was evaluated using MTT assay against HCT 116 cells [31]. HCT 116 cells (1.5×10^5 cells/mL, 100 μL /well) were seeded in 96-wells microtitre plate. Then the plate is incubated in CO_2 incubator for overnight in order to allow the cell for attachment. 100 μL of test substance were added into each well containing the cells. Test substance was diluted with media into the desired concentrations from the stock. The plates were incubated at 37 °C with an internal atmosphere of 5% CO_2 for 72 h. After this treatment period, 20 μL of MTT reagent was added into each well and incubated again for 4 h. After this incubation period, 50 μL of MTT lysis solution (DMSO) was added into the wells. The plates were further incubated for 5 min in CO_2 incubator. Finally, plates were read at 570 and 620 nm wavelengths using a standard ELISA microplate reader. Data were recorded and analyzed for the assessment of the effects of test substance on cell viability. The percentage of growth inhibition was calculated from the optical density (OD) that was obtained from MTT assay, i.e., hundredth multiple of subtracted OD value of control and survived cells over OD of control cells.

2.4. Synthesis

2.4.1. Synthesis of (E)-2-(5-bromo-2-hydroxybenzylidene)-N-methylhydrazinecarbothioamide (1)

A solution of 5-bromo-2-hydroxybenzaldehyde (0.95 g, 4.75 mmol) in ethanol (20 mL) was added to a solution of 4-methyl-3-thiosemicarbazide (0.5 g, 4.75 mmol) in ethanol (20 mL). The resulting yellow solution was refluxed with stirring for 2 h and then filtered. The filtrate was left to stand at room temperature for two days, and plate yellow crystals were obtained. M.p: 185-187 °C. Yield: 1.06 g, 78%. FT-IR (KBr, ν , cm^{-1}): 3398 (s, NH), 3125 (m, OH), 1600 (m, C=N), 1553 (m, C=O), 1271 (m, C=S). ^1H NMR (500 MHz, $\text{DMSO-}d_6$, δ , ppm): 3.01 (s, 3H, CH_3), 6.83-8.15 (m, 3H, Ar-H), 8.28 (q, 1H, CS-NH), 8.57 (s, 1H, CH=N), 11.42 (s, 1H, N-NH). ^{13}C NMR (125 MHz, $\text{DMSO-}d_6$, ppm): 30.80 (CH_3), 111.04-137.01 (C-Ar), 155.44 (C=N), 177.48 (C=S). Anal. calcd. for $\text{C}_9\text{H}_{10}\text{BrN}_3\text{OS}$: C, 37.51; H, 3.50; N, 14.58. Found: C, 37.49; H, 3.45; N, 14.55%.

2.4.2. Synthesis of (E)-2-(2,4-dihydroxybenzylidene)-N-methylhydrazinecarbothioamide (2)

A solution of 2,4-dihydroxybenzaldehyde (0.65 g, 4.75 mmol) in ethanol (20 mL) was added to a solution of 4-methyl-3-thiosemicarbazide (0.5 g, 4.75 mmol) in ethanol (20 mL). The resulting brown solution was refluxed with stirring for 2 h, and then filtered. The filtrate was left to stand at room temperature for two days, and block colorless crystals were obtained. M.p: 198-200 °C. Yield: 0.79 g, 74%. FT-IR (KBr, ν , cm^{-1}): 3351, 3285 (s, NH), 1601 (m, C=N), 1548 (s, C=O), 1273 (m, C=S). ^1H NMR (500 MHz, $\text{DMSO-}d_6$, δ , ppm): 3.01 (s, 3H, CH_3), 6.27-8.25 (m, 3H, Ar-H), 8.30 (q, 1H, CS-NH), 11.41 (s, 1H, N-NH). ^{13}C NMR (125 MHz, $\text{DMSO-}d_6$, ppm): 30.05 (CH_3), 102.28-160.57 (C-Ar), 160.34 (C=N), 177.31 (C=S). Anal. calcd. for $\text{C}_9\text{H}_{11}\text{N}_3\text{O}_2\text{S}$: C, 47.99; H, 4.92; N, 18.65. Found: C, 48.0; H, 4.85; N, 18.68%.

2.4.3. Synthesis of (E)-2-(3-ethoxy-2-hydroxybenzylidene)-N-methylhydrazinecarbothioamide (3)

A solution of 3-ethoxy-2-hydroxybenzaldehyde (0.78 g, 4.75 mmol) in ethanol (20 mL) was added to a solution of 4-methyl-3-thiosemicarbazide (0.5 g, 4.75 mmol) in ethanol (20

mL). The resulting yellow solution was refluxed with stirring for 2 h. A white fluffy product was formed when the solution cooled down to room temperature, then filtered, washed with ethanol and air dried. Plate colorless crystals were obtained by slow evaporation of a DMF solution at room temperature. M.p: 197-199 °C. Yield: 0.92 g, 77%. FT-IR (KBr, ν , cm^{-1}): 3411 (m, NH), 3176 (m, OH), 1598 (s, C=N), 1544 (s, $\text{C}_{\text{aro}}\text{O}$), 1268 (m, C=S). ^1H NMR (500 MHz, $\text{DMSO-}d_6$, δ , ppm): 1.33 (t, 3H, CH_3), 3.01 (s, 3H, CH_3), 4.04 (q, 2H, CH_2), 6.75-7.49 (m, 3H, Ar-H), 8.41 (s, 1H, CH=N), 9.13 (s, 1H, OH), 11.38 (s, 1H, N-NH). ^{13}C NMR (125 MHz, $\text{DMSO-}d_6$, ppm): 14.50 (Ethoxy- CH_3) 30.60 (CH_3), 64.14 (Ethoxy- CH_2), 113.91-146.04 (C-Ar), 146.94 (C=N), 177.39 (C=S). Anal. calcd. for $\text{C}_{11}\text{H}_{15}\text{N}_3\text{O}_2\text{S}$: C, 52.15; H, 5.97; N, 16.59. Found: C, 52.08; H, 5.89; N, 16.59%.

2.4.4. Synthesis of (E)-2-(3-(tert-butyl)-2-hydroxybenzylidene)-N-methylhydrazinecarbothioamide (4)

A solution of 3-ter-butyl-2-hydroxybenzaldehyde (0.84 g, 4.75 mmol) in ethanol (20 mL) was added to a solution of 4-methyl-3-thiosemicarbazide (0.5 g, 4.75 mmol) in ethanol (20 mL). The resulting colorless solution was refluxed with stirring for 2 h and then filtered. The filtrate was left to stand at room temperature; a white product was then collected. Block colorless crystals were obtained by slow evaporation of a DMF solution at room temperature. M.p: 177-179 °C. Yield: 0.95 g, 76%. FT-IR (KBr, ν , cm^{-1}): 3428 (m, NH), 3150 (m, OH), 1599 (s, C=N), 1553 (s, $\text{C}_{\text{aro}}\text{O}$), 1266 (s, C=S). ^1H NMR (500 MHz, $\text{DMSO-}d_6$, δ , ppm): 1.40 (s, 9H, $(\text{CH}_3)_3$), 3.01 (s, 3H, CH_3), 6.87, 7.28 (m, 3H, Ar-H), 8.29 (q, 1H, CS-NH), 8.51 (s, 1H, CH=N), 10.02 (s, 1H, OH), 11.28 (s, 1H, N-NH). ^{13}C NMR (125 MHz, $\text{DMSO-}d_6$, ppm): 29.35 ($(\text{CH}_3)_3$), 31.16 (C $(\text{CH}_3)_3$), 34.45 (CH_3), 118.65-146.64 (C-Ar), 155.19 (C=N), 177.36 (C=S). Anal. calcd. for $\text{C}_{13}\text{H}_{19}\text{N}_3\text{OS}$: C, 58.84; H, 7.22; N, 15.83. Found: C, 58.71; H, 7.16; N, 15.84 %.

2.4.5. Synthesis of (E)-N-methyl-2-(1-(pyridin-2-yl)ethylidene)hydrazinecarbothioamide (5)

A solution of 2-acetyl pyridine (0.57 g, 4.75 mmol) in methanol (20 mL) was added to a solution of 4-methyl-3-thiosemicarbazide (0.5 g, 4.75 mmol) in methanol (20 mL). The resulting solution was refluxed with stirring for 2 h. A white product was formed when the solution cooled down to room temperature, then filtered, washed with ethanol and air dried. Block colorless crystals were obtained by slow evaporation of a DMF solution at room temperature. M.p: 187-189 °C. Yield: 0.80 g, 81%. FT-IR (KBr, ν , cm^{-1}): 3301 (m, NH), 3146 (m, OH), 1601 (m, C=N), 1557 (s, $\text{C}_{\text{aro}}\text{O}$), 1269 (m, C=S). ^1H NMR (500 MHz, $\text{DMSO-}d_6$, δ , ppm): 2.35 (s, 3H, CH_3), 3.01 (s, 3H, CH_3), 7.38, 7.83, 8.39, 8.55 (m, 4H, Ar-H), 8.65 (q, 1H, CS-NH), 10.28 (s, 1H, N-NH). ^{13}C NMR (125 MHz, $\text{DMSO-}d_6$, ppm): 12.06 (CH_3), 31.10 (N- CH_3), 120.76-148.43 (C-Ar), 154.52 (C=N), 178.50 (C=S). Anal. calcd. for $\text{C}_9\text{H}_{12}\text{N}_4\text{S}$: C, 51.90; H, 5.81; N, 26.90. Found: C, 51.21; H, 5.72; N, 26.81%.

3. Results and discussion

3.1. Chemistry

New thiosemicarbazones (1-5) have been prepared through the condensation of corresponding salicylaldehyde derivatives or 2-acetylpyridine and *N*(4)-methylthiosemicarbazide [32]. All the compounds are air-stable and highly soluble in DMSO and DMF. Moreover, the compounds are insoluble and highly stability in aqueous solutions. ^1H NMR and UV spectra were recorded after preparation, 7 days, 15 days, 30 days, 3 months and 6 months, while kept at room temperature. All spectra confirmed the stability of the prepared compounds in aqueous solutions. Compounds identity was determined by ^1H NMR, ^{13}C NMR and elemental

analysis which are confirmed their assigned structures. The compounds 1-5 exhibited well-resolved single crystals, FT-IR, ^1H NMR, and ^{13}C NMR spectra and elemental analysis characteristics consistent with their assigned structures.

In FT-IR, the bands in the 1598 to 1610 cm^{-1} range can be attributed to the (C=N) group, the bands in the 1544 to 1553 cm^{-1} range can be attributed to the ($\text{C}_{\text{aro}}\text{O}$) group, and the bands in the 1267 to 1273 cm^{-1} range can be attributed to the C=S group.

In the ^1H NMR, the signal caused by the protons of the terminal (CH_3) group is emerged at δ 3.01 ppm. The signal caused by the proton of CS-NH group is emerged at the range from δ 8.28 to 8.37 ppm. The aromatic protons signals are observed from δ 6.27 to 8.25 ppm. The signal from δ 8.41 to 9.13 ppm is attributed to the proton of CH=N group, whereas the signals from δ 11.38 to 11.77 ppm is attributed to the proton of N-NH group.

In the ^{13}C NMR, the signals from δ 177.31 to 179.16 ppm are attributed to the carbon of C=S group. The carbon signal of C=N group is appeared from δ 146.94 to 160.34 ppm, and the signals of aromatic carbons are appeared from δ 111.04 to 144.58 ppm.

3.2. Crystal and molecular structures

Crystal and molecular structures of the compounds 1-5 were obtained using crystal X-ray diffraction. The general crystal data are listed in Table 1, the relevant bond distances and angles are shown in Table 2, and their molecular structures are shown in Figures 1-5.

The compound 2 is a second monoclinic ($P2_1/c$) polymorph of the previously reported *Cc* form [33]. The molecule is non-planar, with dihedral angle between the N_3CS residue and the benzene ring being 21.35(4) °. The conformation about the C=N bond (1.291(2) Å) is *E*, the two N-bound H atoms are *anti*, and the inner hydroxyl O-bound and outer amide N-bound H atoms form intramolecular hydrogen bonds to the imine N atom. Crucially, the H atom of the outer hydroxyl group is approximately *syn* to the H atom of the benzene C atom connecting the two C atoms bearing the hydroxyl substituents. This arrangement enables the formation of supramolecular tubes aligned along [010] and sustained by N-H...O, O-H...S and N-H...S hydrogen bonds; the tubes pack with no specific interactions between them. While the molecular structure in *Cc* form is comparable, the H atom of the outer hydroxyl group is approximately *anti* rather than *syn*. This different orientation leads to the formation a three-dimensional architecture based on N-H...O and O-H...S hydrogen bonds [34].

The molecular structures of compounds 1-5 showed different configurations according their structural geometries and elements symmetry. In the compound 1, 2 and 4, the N1 atom show the *trans* geometry in relation to C5 atom, and *cis* geometry in relation to C1 atom. These geometries allow the formation of intrahydrogen bonding between N1 atom and O1 atom. In the compound 3, the aromatic ring rotates approximately 180 ° around the N1-C7 bond which leads to change the *trans* geometry to *cis* geometry between N1 atom and C5 atom (corresponded to C1 in compound 1, 2 and 4), as well as the *cis* geometry to *trans* geometry between N1 atom and C1 atom (corresponded to C5 atom in compound 1, 2 and 4). These geometries prevent the formation of intrahydrogen bonding between N1 and O1. Furthermore, the compounds 1-4 show the *trans* geometries between N1 atom and S1 atom as well as between C9 atom and N2 atom, and *cis* geometries between N1 atom and N2 atom as well as between C9 atom and S1 atom.

The compound 4 was reported in our previous work but has not been isolated as a single crystal [35]. The asymmetric unit of the compound 4 contains three, A, B and C, $\text{C}_{13}\text{H}_{19}\text{N}_3\text{OS}$ and three $\text{C}_3\text{H}_7\text{NO}$ solvent molecules. Such crystallographically different units have been rarely isolated [36].

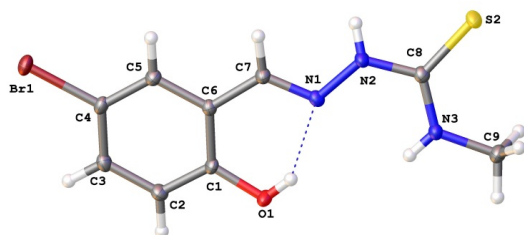
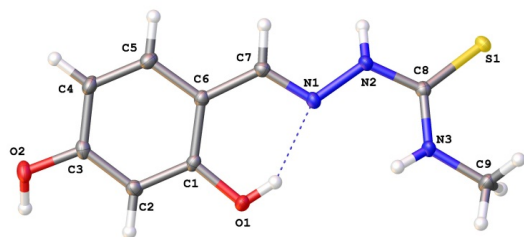
Table 1. Crystallographic data of compounds 1-5.

Parameter	1	2	3	4	5
Chemical formula	C ₉ H ₁₀ BrN ₃ OS	C ₉ H ₁₁ N ₃ O ₂ S	C ₁₁ H ₁₅ N ₃ O ₂ S	C ₁₃ H ₁₆ N ₃ OS, C ₃ H ₇ NO	C ₉ H ₁₂ N ₄ S
Formula weight	288.17	225.28	253.33	338.48	208.30
Crystal system	Monoclinic	Monoclinic	Monoclinic	Triclinic	Monoclinic
Crystal description	Plate yellow	Block colorless	Plate colorless	Block colorless	Block colorless
Space group	P2 ₁ /c	P2 ₁ /c	P2 ₁ /c	P-1	P2 ₁ /c
a (Å)	8.3776(1)	7.3058(2)	14.3413(7)	12.4996(2)	8.7849(3)
b (Å)	6.2010(1)	6.0582(1)	6.0078(3)	13.4853(2)	7.5662(3)
c (Å)	21.1050(3)	22.6041(6)	16.2414(7)	17.1744(2)	15.4579(5)
α (°)	90	90	90	99.975(1)	90
β (°)	94.552(1)	91.100(2)	117.557(3)	93.220(1)	105.734(2)
γ (°)	90	90	90	106.833(1)	90
Volume (Å ³)	1092.94(3)	1000.27(4)	1240.60(11)	2711.59(7)	988.96(6)
Z	4	4	4	6	4
D _{calc} (g/cm ³)	1.822	1.496	1.356	1.244	1.399
Crystal size (mm)	0.07 × 0.29 × 0.45	0.41 × 0.19 × 0.48	0.08 × 0.16 × 0.65	0.15 × 0.24 × 0.46	0.22 × 0.33 × 0.40
Temperature (K)	100	100	100	100	100
Total data	22785	11216	12899	58926	13353
Unique data	4831	2939	3287	15795	3598
R _{int}	0.030	0.029	0.049	0.066	0.029
Observed data [I>2σ(I)]	3856	2389	2224	9130	3052
R ₁	0.0307	0.0391	0.0474	0.0694	0.0372
wR ₂	0.0694	0.0974	0.1058	0.1423	0.0901
s	1.07	1.05	1.04	1.03	1.06

Table 2. Selected bond length (Å) and angles (°) for the compounds 1-5.

Compound	1	2	3	4A	4B	4C	5
Bond distances (Å)							
N2-C8	1.3585(19)	1.3627(19)	1.359(3)	1.355(3)	1.354(3)	1.356(3)	1.3684(14)*
S1-C8	1.6885(14)	1.7001(13)	1.693(2)	1.700(2)	1.695(2)	1.698(2)	1.6897(11)*
N1-N2	1.3801(18)	1.3934(17)	1.376(2)	1.383(3)	1.384(3)	1.380(3)	1.3752(14)*
N3-C8	1.3287(18)	1.3234(18)	1.326(3)	1.322(3)	1.323(3)	1.356(3)	1.3296(14)*
N3-C9	1.455(2)	1.459(2)	1.451(3)	1.454(3)	1.453(3)	1.448(3)	1.4572(14)*
N1-C7	1.2880(19)	1.2927(18)	1.284(3)	1.287(3)	1.283(3)	1.288(3)	1.2927(14)*
Bond angles (°)							
N1-N2-C8	121.89(12)	120.32(11)	120.43(17)	122.17(18)	121.67(18)	121.78(18)	118.48(9)
S1-C8-N3	75.47(11)	118.02(12)	124.49(18)	123.16(18)	123.51(17)	123.30(18)	123.61(8)
S1-C8-N2	118.04(10)	117.98(10)	119.50(15)	118.55(16)	118.70(16)	118.56(15)	119.63(8)
C8-N3-C9	123.35(13)	124.57(13)	124.29(19)	122.6(2)	123.0(2)	123.2(2)	123.29(10)
N2-N1-C7	114.26(12)	113.65(11)	115.28(16)	114.55(17)	114.89(17)	114.93(17)	117.77(9)

* For 5; N1=N2, N2=N3, N3=N4, C8=C7 and C7=C6.

**Figure 1.** Molecular structure of compound 1.**Figure 2.** Molecular structure of compound 2.

The molecular structures show the 4A and 4B have the same conformations and the 4C is enantiomer. Therefore, the 4A and 4B show the *anti*-conformation of the N1 atom with respect to S1 atom [Torsion angle N1A-N2A-C8A-S1A = -176.37(15)° and torsion angle N1B-N2B-C8B-S1B = -172.53(15)°], O1 atom with respect to C3 atom [Torsion angle O1A-C1A-C2A-C3A = -179.23(18)° and torsion angle O1B-C1B-

C2B-C3B = -179.24(18)°], whereas 4C shows the *syn*-conformations (Torsion angle N1C-N2C-C8C-S1C = 175.89(15)° and torsion angle O1C-C1C-C2C-C3C = 178.76(19)°). In addition, 4A and 4B show the *syn*-conformation of the C9 atom with respect to S1 atom (Torsion angle C9A-N3A-C8A-S1A = 2.3(3)° and torsion angle C9B-N3B-C8B-S1B = 4.0(3)°), C1 atom with respect to C11 atom (Torsion angle C1A-C2A-C10A-C11A = 177.41(9)° and torsion angle C1B-C2B-C10B-C11B = 178.6(2)°), whereas 4C shows the *anti*-conformations (Torsion angle C9C-N3C-C8C-S1C = -3.8(3)° and torsion angle C1C-C2C-C10C-C11C = -177.7(2)°). In the compound 5, the N2 atom shows the *trans* geometries in relation to N1 atom and S1 atom, as well as the N3 atom shows the *trans* geometries in relation to C5 atom and terminal C8 atom. Furthermore, the *cis* geometries appear between S1 atom and C8 atom as well as between N1 atom and C9 atom which is occupy the apical position. Moreover, the N2-C8 and C8-S1 bond distances indicate the thione form for all the compounds, which has been changed to thiol form upon complexation [37].

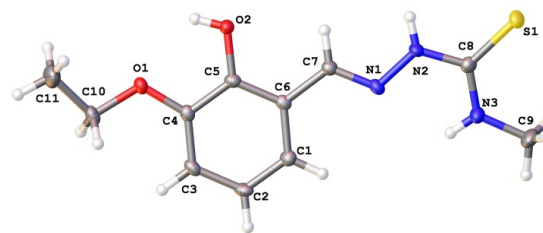
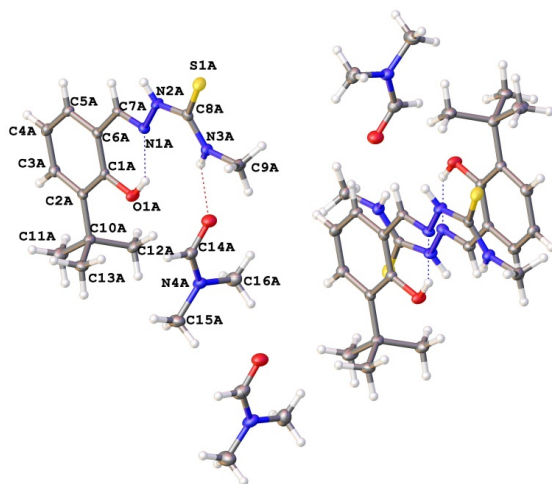
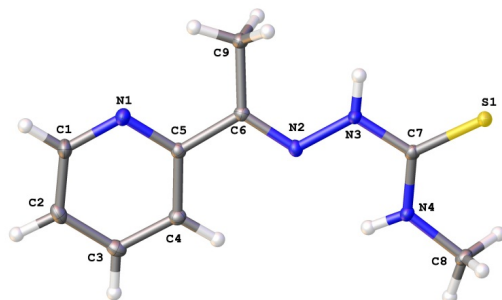
**Figure 3.** Molecular structure of compound 3.

Table 3. Selected hydrogen bonds parameters of the compounds 1-5 (Å and °).

Compound	D-H...A	Symmetry	d(D-H)	d(H...A)	d(D...A)	<(DHA)
1	N3-H...N1		0.77(2)	2.40(2)	2.7242(18)	106.8(18)
	N2-H...O1	$x, -1+y, z$	0.81(2)	2.29(3)	3.0579(17)	3.0579(17)
	O1-H...N1		0.76(3)	2.02(3)	2.6809(17)	146(3)
2	N2-H...O1	$x, 1+y, z$	0.90(2)	2.08(2)	2.9531(17)	162(2)
	N3-H...S1	$x, -1+y, z$	0.822(19)	2.758(18)	3.3877(13)	134.8(17)
	N3-H...N1		0.822(19)	2.35(2)	2.7074(18)	106.8(16)
3	N2-H...O2	$1-x, 2-y, 2-z$	0.85(2)	2.16(2)	2.955(2)	155(2)
	N3-H...N1		0.83(2)	2.23(3)	2.639(3)	111(2)
	O2-H...O1		0.82(3)	2.16(2)	2.619(2)	115(2)
	O2-H...S1	$1-x, 2-y, 2-z$	0.82(3)	2.52(3)	3.2107(17)	142(2)
4	N2A-H...S1B	$2-x, 1-y, -z$	0.84(3)	2.55(3)	3.3670(19)	166(2)
	N2B-H...S1A	$2-x, 1-y, -z$	0.84(2)	2.58(2)	3.3989(19)	166(2)
	N3B-H...O2B	$1+x, y, z$	0.87(2)	2.18(2)	2.918(3)	143(2)
	N2C-H...S1C	$x, 1+y, z$	0.89(3)	2.50(3)	3.3675(19)	165(2)
5	N4-H...N2		0.857(17)	2.242(17)	2.6302(14)	107.5(13)
	N4-H...S1	$2-x, -1/2+y, 1/2-z$	0.857(17)	2.769(16)	3.4594(10)	138.7(14)
	N3-H...S1	$2-x, 2-y, -z$	0.865(16)	2.715(16)	3.5487(10)	162.5(13)

**Figure 4.** Molecular structure of compound 4. Molecular structures of A, B and C.**Figure 5.** Molecular structure of compound 5.

From the other hand, the crystal structure of the compound 1-5 form centrosymmetrically related dimmers through the intermolecular hydrogen bonds; their parameters are listed in Table 3.

3.3 Interaction with DNA

3.3.1. Electronic absorption studies

Electronic absorption is one of the most useful methods in DNA binding studies [38,39]. Compounds bind to DNA through covalent bonding [40] or noncovalent interaction, such as intercalation, electrostatic binding, or groove binding [41].

Absorption spectroscopic studies were carried out on a spectrophotometer (Perkin Elmer, Lambda-35), using fixed concentrations of the ligand (50 μM) with increasing amounts of DNA from 28.9 μM to 173.4 μM in 6.3 mM Tris-HCl/50 mM NaCl buffer (pH = 7). Each addition left for equilibrium at 25 $^{\circ}\text{C}$ for 10 min. and scanned from 230 to 600 nm. All the compounds revealed two absorption bands attributed to the $\pi \rightarrow \pi^*$ and $n \rightarrow \pi^*$ transitions at 305 and 338 nm, respectively. The $\pi \rightarrow \pi^*$ absorption bands were used to observe the interaction of CT-DNA with compounds. The observed spectral behavior suggest intercalative interaction to DNA [42], which lead to hypochromism in spectral bands with increasing DNA concentration (Figure 6). The change in absorbance was used to estimate the intrinsic binding constant K_b at 305 nm using the following equation (1) [43]:

$$[\text{DNA}] / (\varepsilon_a - \varepsilon_f) = [\text{DNA}] / (\varepsilon_b - \varepsilon_f) + 1/K_b (\varepsilon_b - \varepsilon_f) \quad (1)$$

where the absorption coefficients ε_a , ε_f and ε_b correspond to $A_{\text{abs}}/[\text{DNA}]$, the extinction coefficient for the free compound, and the extinction coefficient for the ligand in fully bound form, respectively. The plot of $[\text{DNA}]/(\varepsilon_a - \varepsilon_f)$ versus $[\text{DNA}]$ gives a slope $1/(\varepsilon_a - \varepsilon_f)$ and intercept $1/K_b (\varepsilon_b - \varepsilon_f)$ as shown in Figure 7.

The binding constants (Table 4) suggest that all the compounds are strongly bind to the CT-DNA. The K_b values shows that the binding strength follow the order, $4 > 5 > 1 > 2 > 3$. In addition of an influence of the terminal methyl group, the presence of *tert*-butyl group provides a strong lipophilic or hydrophobic medium which enables the compound 4 ($K_b = 1.834 \times 10^5 \text{ M}^{-1}$) to move into the hydrophobic medium of DNA and consequently moves rapidly between the DNA bases which in turn bind strongly with DNA compared to the compound 5 ($K_b = 1.662 \times 10^5 \text{ M}^{-1}$) that have one methyl group. The polarized bromine moiety increases the London dispersion forces and consequently increases the lipophilic properties which makes the compound 1 ($K_b = 8.791 \times 10^4 \text{ M}^{-1}$) a strong intercalator. Moreover, the binding strength is depends on the planarity of the compounds which provided by the geometrical and conformational structures, a strong intercalator that have more planarity [44]. The compound 3 showed different geometrical structures than the other compounds as mentioned the crystal section, and may be responsible about the binding strength of this compound as well as the presence of the withdrawing ethoxy group compared to donating hydroxyl group which is makes the compound 2 ($K_b = 6.551 \times 10^4 \text{ M}^{-1}$) a good intercalator than compound 3 ($K_b = 4.873 \times 10^4 \text{ M}^{-1}$). Furthermore, the binding of the compounds to CT DNA caused isosbestic spectral changes with an isosbestic points at 289 nm. The presence of isosbestic points are attributed to the increasing concentration of DNA which leads to increasing absorbance in this region.

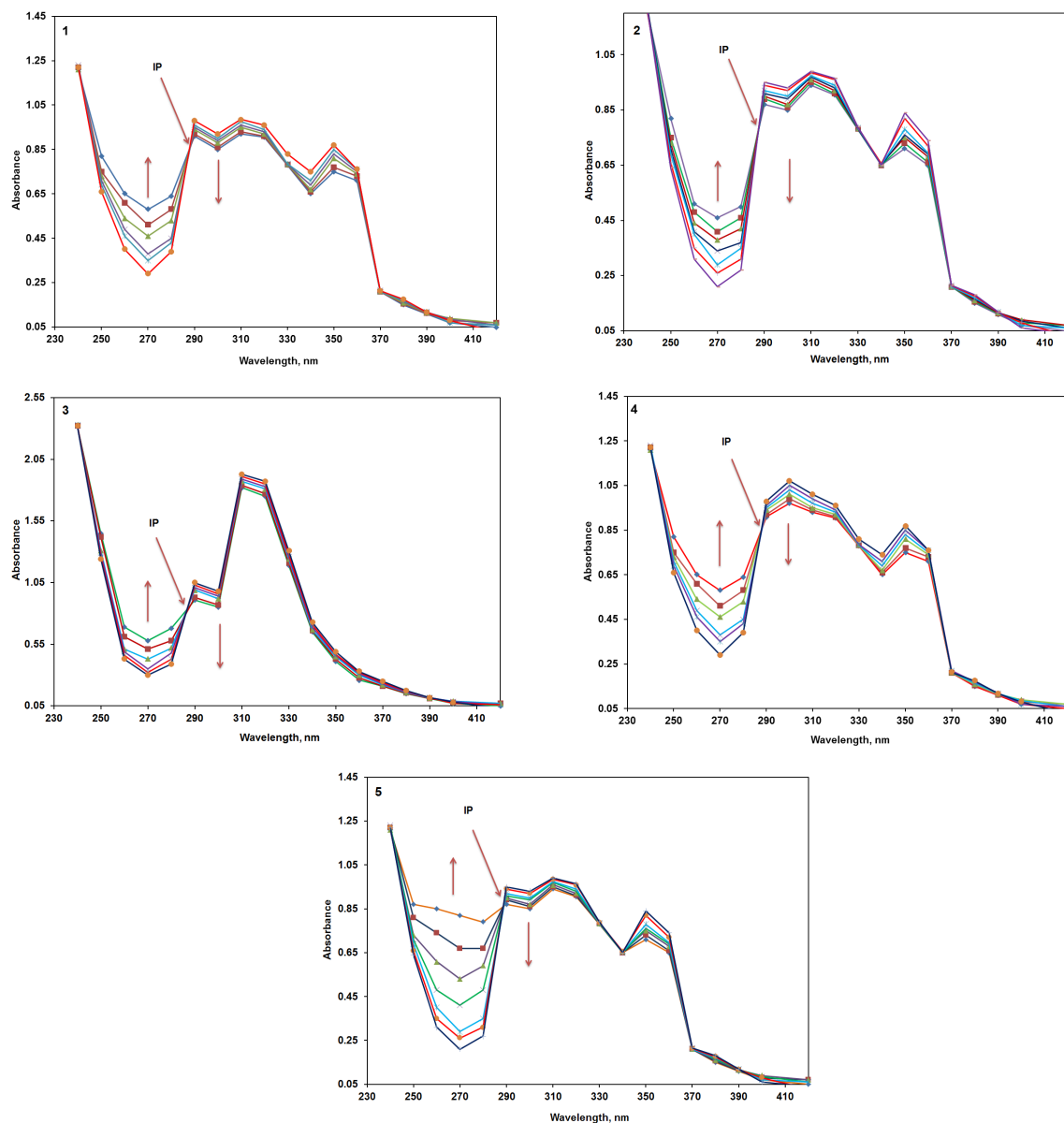


Figure 6. UV spectra of the compounds 1-5, in 6.3 mM Tris-HCl/50 mM NaCl buffer (pH = 7) in presence of CT-DNA at increasing amounts. [Compound] = 50 μ M, [DNA] = (28.9-173.4) μ M. The arrows show the changes in absorbance upon increasing amounts of CT-DNA. IP = Isosbestic point.

3.3.2. Fluorescence emission studies

Emission spectral studies were carried out in order to evaluation the changes that accompany the CT-DNA additions on the fluorescence spectra of the synthesized compounds. The fluorescence emission is due to return the molecules to the electronic ground state π from the electronic excited state π^* rather than the $n \rightarrow \pi^*$ transition because the quantum efficiency is greater and the lifetime is shorter than that for the $n \rightarrow \pi^*$ transition [45]. The compounds 2, 3 and 5 showed two fluorescence emission at 380 nm and at longer wavelength, 500 nm, due to isosbestic spectral changes with an isosbestic points at 408 nm, presumably due to formation of excimer (Figure 8). The isosbestic points are not commonly appear in fluorescence spectra, anyway, the presence of isosbestic point is attributed to the rigidity and steric features that succeed to bring the molecules close enough which assist to generate an excimer molecule.

In the compound 2, the presence of hydroxyl substituent on aromatic ring decreases the intensity of the monomeric fluorescent peak at 380 nm, which suggest that the probability of intersystem crossing increases depending on the molar mass of the substituent. By contrast, the presence of ethoxy and methyl moieties increases the intensity of the monomeric fluorescent peak at 380 nm of compound 3 and 5, respectively, due to increases the rigidity via the formation of hydrogen bonding [46]. The compound 1 showed three emission peaks at 380 nm back to the monomeric molecule, 500 nm back to the first excimer molecule and 760 nm back to the second excimer molecule. In general, the fluorescence emission decreases upon addition of CT-DNA which confirms the intercalative binding between the compounds and DNA. From the other hand, the CT-DNA addition to the compounds decreases the intensity of the excimer fluorescent peaks at 500 nm and increases the intensity of the monomeric fluorescent peaks at 380 nm.

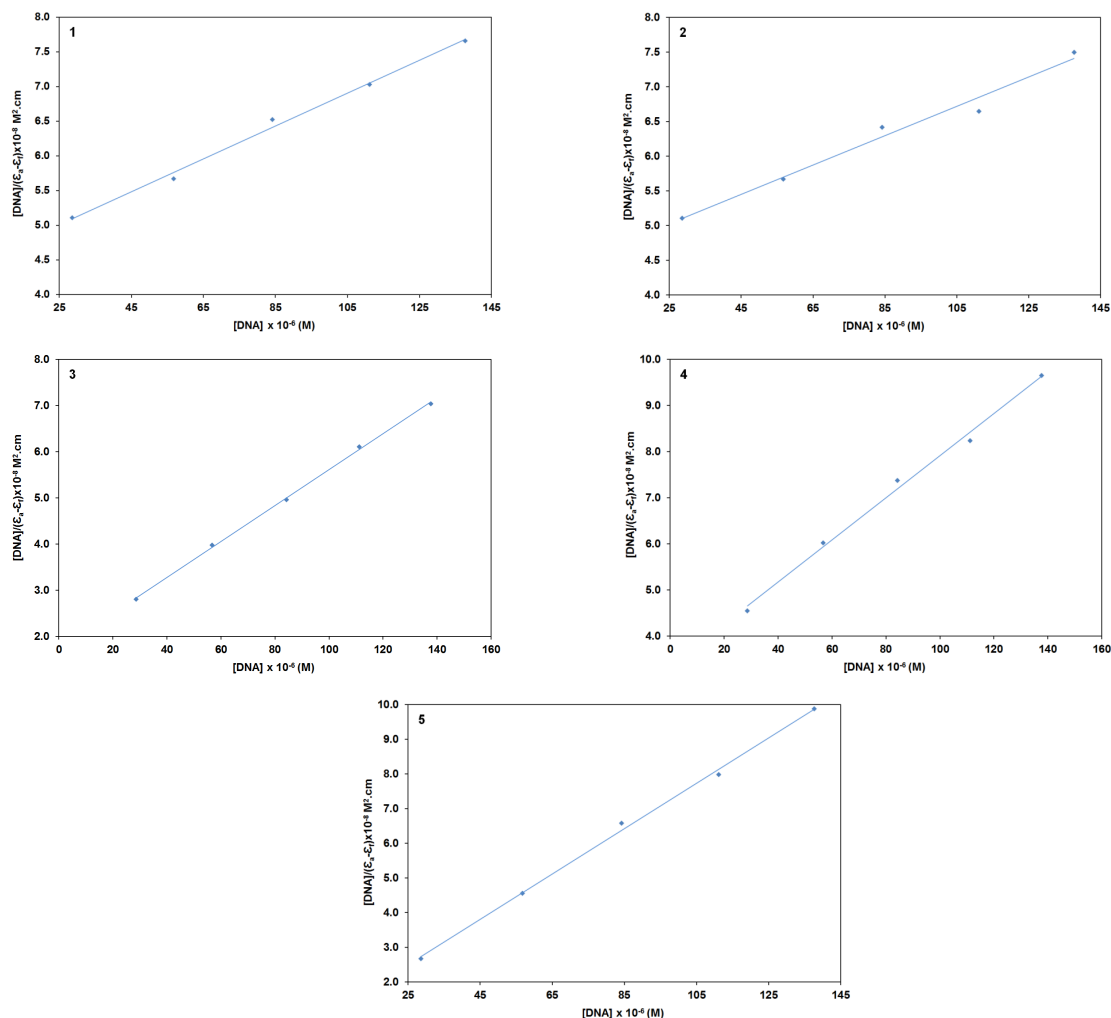


Figure 7. Plots of $[DNA]/(\epsilon_a - \epsilon_i)$ vs $[DNA]$.

These changes are suggest that the interaction occurs between the excimer molecule and DNA and hence separate the monomer molecule which leads to increases the fluorescence intensity at 380 nm [47]. The compound 4 shows one fluorescence emission at 380 nm, which is the intensity decreases upon addition the DNA to the ligand.

3.3.3. Viscosity measurement

Viscosity assays are regarded as one of the most important tests for assessing the binding modes of compounds to DNA. Intercalation of compounds into DNA increases the viscosity because of the extension and stiffening of the DNA helix [48]. The viscometric studies were performed by adding increasing amounts of the compounds to fixed amount of CT DNA at 37 °C in 6.3 mM Tris-HCl/50 mM NaCl buffer (pH = 7). The corresponding results are shown in Figure 9. These results confirm the intercalative binding and support the spectrometric results.

3.4. Antiproliferative activity

Antiproliferation tests were performed *in vitro* on human colorectal cancer (HCT 116) cell line. The compounds showed a pronounced activity than the standard reference, 5-fluorouracil (median inhibitory concentration $[IC_{50}] = 7.3 \mu\text{M}$).

The IC_{50} values of the tested compounds (Table 4) showed that the order of antiproliferative efficiency was $4 > 5 > 1 > 2 > 3$.

Table 4. DNA binding constants (K_b) and IC_{50} of compounds 1-5.

Compound	$K_b \text{ (M}^{-1}\text{)}$	$IC_{50} \text{ (}\mu\text{M)}$
1	8.791×10^4	4.1
2	6.551×10^4	4.5
3	4.873×10^4	6.3
4	1.834×10^5	3.3
5	1.662×10^5	3.5
5-FU	-	7.3

These results are consistent with those obtained for DNA binding and confirm that the compound activity is dependent on the substituent of the aromatic ring, a 100 μM 4, 5, 1, 2 and 3 is sufficient to inhibit 97.6, 95.6, 85.9, 70.2 and 62.0% cell proliferation, respectively (Figure 10). Figure 11 shows the HCT 116 cell images after 48 h of treatment with the compounds. These images were taken with inverted phase-contrast microscopy at $\times 200$ magnification and a digital camera at 48 h after treatment of the samples. The analysis of the photomicrographs shows that the compounds generally showed apoptotic features in the affected cells. The blabbing of the cell membrane and vesicle formation in the treated cells indicate the unique characteristics of apoptosis.

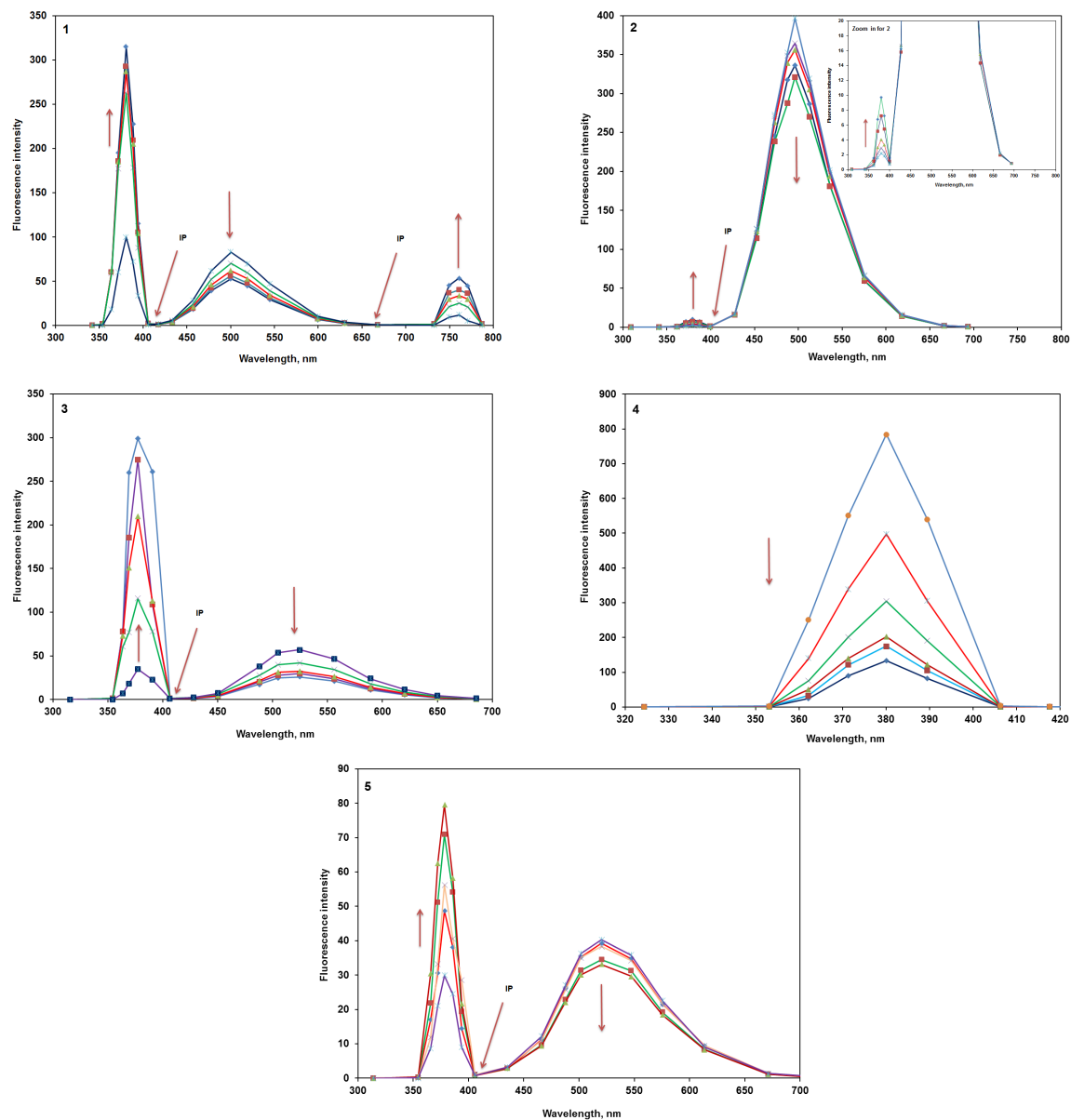


Figure 8. Fluorescence spectra of the compounds 1-5, in 6.3 mM Tris-HCl/50 mM NaCl buffer (pH = 7) in presence of CT-DNA at increasing amounts. [Compound] = 50 μ M, [DNA] = (28.9-173.4) μ M. The arrows show the changes in fluorescence intensity upon increasing amounts of CT-DNA. IP = Isosbestic point.

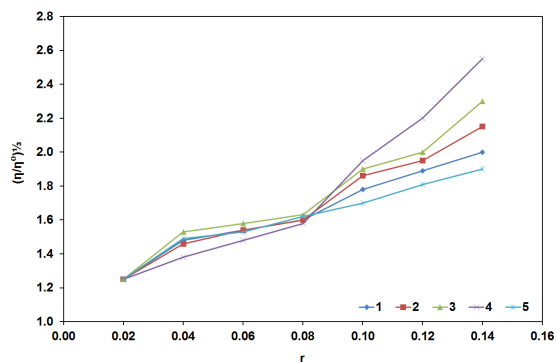


Figure 9. Viscometric results of the compounds 1-5, in 6.3 mM Tris-HCl/50 mM NaCl buffer (pH = 7) in presence of CT-DNA and increasing amounts of compound at 37 $^{\circ}$ C; $r = [\text{Compound}]/[\text{DNA}]$.

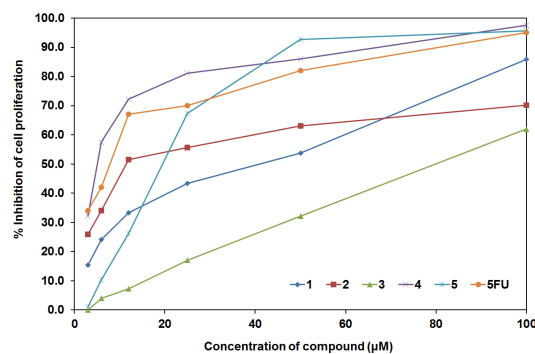


Figure 10. Cell proliferation inhibition by the compounds 1-5 at concentration range 3.0, 6.0, 12, 25, 50 and 100 µM using 5-FU as a reference.

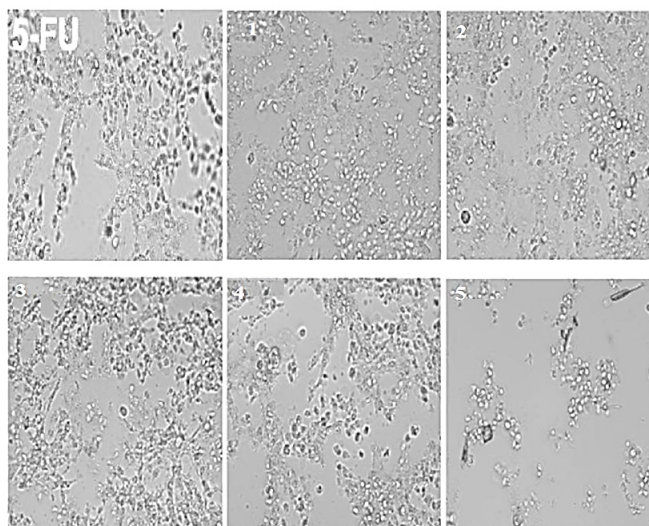


Figure 11. Photomicrographs of the HCT 116 cell lines after treatment with the compounds and 5-FU as standard reference.

4. Conclusions

Five new thiosemicarbazones derivatives were synthesized, characterized and structurally identified using X-ray crystallographic technique. Compound **4** revealed rarely observed crystallographically different three units of the same molecule which have slightly different bond lengths and angles. Such crystallographically different units have been rarely isolated. The binding strength of compounds with CT-DNA as well as their antiproliferative activity against human colorectal cancer (HCT 116) cell line has been evaluated. The results showed the intercalation interaction between the compounds and DNA. The compounds **4** and **5** showed more pronounced binding strength as well as cytotoxic properties and found to have considerable antiproliferative abilities than compared to compound **1**, **2** and **3**. The current study revealed that the terminal N(4)-methyl group and the substituent methyl groups on aromatic ring are more increased the binding strength compared to bromine group. Furthermore, the presence of donating group on aromatic ring increases the strength of intercalator compared to the presence of withdrawing group. Moreover, the study revealed that the binding strength depends on the planarity that provided by the geometrical and conformational structures of compound.

Acknowledgements

We thank the Universiti Sains Malaysia and the Malaysian Government for a Research Grant which partly supported this work.

Supplementary materials

CCDC 885706, 960620, 953516, 949331 and 949332 contain the supplementary data for compound **1**, **2**, **3**, **4** and **5**, respectively. These data can be obtained free of charge at http://www.ccdc.cam.ac.uk/data_request/cif.

References

- Adeline, Y. L.; Danuta, S. K.; Naresh, K.; Des, R. R. *Org. Biomol. Chem.* **2013**, *11*, 6414-6425.
- Kalaivani, P.; Prabhakaran, R.; Ramachandran, E.; Dallemer, F.; Paramaguru, G.; Renganathan, R.; Poornima, P.; Vijaya Padma, V.; Natarajan, K. *Dalton Trans.* **2012**, *41*, 2486-2499.
- Afrasiabi, Z.; Sinn, E.; Kulkarni, P. P.; Ambike, V.; Padhye, S.; Deobagakar, D.; Heron, M.; Gabbutt, C.; Anson, C. E.; Powell, A. K. *Inorg. Chim. Acta* **2005**, *358*, 2023-2030.
- Sampath, K.; Sathiyaraj, S.; Raja, G.; Jayabalakrishnan, C. *J. Mol. Struct.* **2013**, *1046*, 82-91.
- Ngan, N. K.; Lo, K. M.; Wong, C. S. R. *Polyhedron* **2012**, *33*, 235-251.
- Eierhoff, D.; Tung, W. C.; Hammerschmidt, A.; Krebs, B. *Inorg. Chim. Acta* **2009**, *362*, 915-298.
- Tarlok, S. L.; Rekha, S.; Gagandeep, B.; Sonia, K. *Coord. Chem. Rev.* **2009**, *253*, 977-1055.
- Casas, J. S.; Garcia, T. M. S.; Sordo, J. *Coord. Chem. Rev.* **2000**, *209*, 197-261.
- Liberta, A. E.; West, D. X. *Biometals* **1992**, *5*, 121-126.
- Lobana, T. S.; Khanna, S.; Butcher, R. J.; Hunter, A. D.; Zeller, M. *Inorg. Chem.* **2007**, *46*, 5826-5828.
- Lobana, T. S.; Kumari, P.; Butcher, R. J. *Inorg. Chem. Comm.* **2008**, *11*, 11-14.
- Pedrido, R.; Berbejo, M. R.; Romero, M. J.; Vazquez, M.; Gonzales-Noya, A. M.; Maneiro, M.; Rodrique, M. J.; Fernandez, M. I. *Dalton Trans.* **2005**, *3*, 572-579.

- [13]. Labisbal, E.; Haslow, K. D.; Sousa-Pedrares, A.; Valdes-Martinez, J.; Harnandez-Ortega, S.; West, D. X. *Polyhedron* **2003**, *22*, 2831-2837.
- [14]. Ashfield, L. J.; Cowley, A. R.; Dilworth, J. R.; Donnelly, P. S. *Inorg. Chem.* **2004**, *43*, 4121-4123.
- [15]. Lobana, T. S.; Bawa, G.; Butcher, R. J.; Liaw, B. J.; Liu, C. W. *Polyhedron* **2006**, *25*, 2897-2903.
- [16]. Zeglis, B. M.; Divilov, V.; Lewis, J. S. *J. Med. Chem.* **2011**, *54*, 2391-2398.
- [17]. Hall, M. D.; Brimacomble, K. R.; Varonka, M. S.; Pluchino, K. M.; Monda, J. K.; Walsh, M. J.; Boxer, M. B.; Warren, T. H.; Fales, H. M.; Gottesman, M. M. *J. Med. Chem.* **2011**, *54*, 5878-5889.
- [18]. Kowol, C. R.; Berger, R.; Eichinger, R.; Roller, A.; Jakupec, M. A.; Schmidt, P. P.; Arion, V. B.; Keppler, B. K. *J. Med. Chem.* **2007**, *50*, 1254-1265.
- [19]. Kalaivani, P.; Prabhakaran, R.; Poornima, P.; Dallemer, F.; Vijayalakshmi, K.; Vijaya Padma, V.; Natarajan, K. *Organometallics* **2012**, *31*, 8323-8332.
- [20]. Hussein, M. A.; Guan, T. S.; Haque, R. A.; Ahamed, M. B. K.; Majid, A. M. S. A. *J. Coord. Chem.* **2014**, *67*, 714-727.
- [21]. Richards, A. D.; Rodger, A. *Chem. Soc. Rev.* **2007**, *36*, 471-483.
- [22]. Hartwig, A. *Chem. Biol. Interact.* **2010**, *184*, 269-272.
- [23]. Hussein, M. A.; Guan, T. S.; Haque, R. A.; Ahamed, M. B. K.; Majid, A. M. S. A. *Polyhedron* **2015**, *85*, 93-103.
- [24]. Seena, E. B.; Prathapachandra Kurup, M. R. *Polyhedron* **2007**, *26*, 3595-3601.
- [25]. Ramachandran, E.; Senthil Raja, D.; Bhuvanesh, N. S.; Natarajan, K. *Dalton Trans.* **2012**, *41*, 13308-13323.
- [26]. Panchangam, M. K.; Katreddi, H. R. *Inorg. Chim. Acta* **2009**, *362*, 4185-4190.
- [27]. Hussein, M. A.; Iqbal, M. A.; Asif, M.; Haque, R. A.; Ahamed, M. B. K.; Majid, A. M. S. A. Guan, T. S. *Phosphorus, Sulfur Silicon Relat. Elem.* **2015**, *190*, 1498-1508.
- [28]. Sheldrick, G. M. *Acta Cryst. A* **2008**, *64*, 112-122.
- [29]. Ali, A. Q.; Teoh, S. G.; Eltayeb, N. E.; Ahamed, M. B. K.; Majid, A. M. S. A. *Polyhedron* **2014**, *74*, 6-15.
- [30]. Skyrianou, K. C.; Perdih, F.; Papadopoulos, A. N.; Turel, I.; Kessissoglou, D. P.; Psomas, G. *J. Inorg. Biochem.* **2011**, *105*, 1273-1285.
- [31]. Mosmann, T. J. *Immunol. Methods* **1983**, *65*, 55-63.
- [32]. Vrdoljak, V.; Cindric, M.; Milic, D.; Matkovic-Calogovic, D.; Novak, P.; Kamenar, B. *Polyhedron* **2005**, *24*, 1717-1726.
- [33]. Tan, K. W.; Ng, C. H.; Maah, M. J.; Ng, S. W. *Acta Crystallogr E* **2008**, *64*, o2224-o2231.
- [34]. Salam, M. A.; Hussein, M. A.; Tiekink, R. T. *Acta Crystallogr E* **2015**, *71*, 58-71.
- [35]. Hussein, M. A.; Guan, T. S.; Haque, R. A.; Ahamed, M. B. K. Majid, A. M. S. A. *Spectrochim. Acta A* **2015**, *136*, 1335-1348.
- [36]. Vandresen Falzirolli, H.; Almeida Batista, S. A.; da Silva-Giardini, A. P. B.; da Oliveira, D. N.; Catharino, R. R.; Ruiz, A. L. T. G.; de Carvalho, J. E.; Foglio, M. A. da Silva, C. C. *Eur. J. Med. Chem.* **2014**, *79*, 110-116.
- [37]. Hussein, M. A.; Guan, T. S.; Haque, R. A.; Ahamed, M. B. K. Majid, A. M. S. A. *Inorg. Chim. Acta* **2014**, *421*, 270-283.
- [38]. Chao, H.; Mei, W.; Huang, Q.; Ji, L. *J. Inorg. Biochem.* **2002**, *92*, 165-170.
- [39]. Kamatchi, T. S.; Chitrapriya, N.; Kim, S. K.; Fronczek, F. R.; Natarajan, K. *Eur. J. Med. Chem.* **2013**, *59*, 253-264.
- [40]. Sherman, S. E.; Gibson, D.; Wang, A. H. J.; Lippard, S. J. *J. Am. Chem. Soc.* **1988**, *110*, 7368-7381.
- [41]. Strekowski, L.; Wilson, B. *Mutat. Res.* **2007**, *623*, 3-13.
- [42]. Richards, A. D.; Rodgers, A. *Chem. Soc. Rev.* **2007**, *36*, 471-483.
- [43]. Liu, F. R.; Wang, K. Z.; Bai, G. Y.; Zhang, Y. A.; Gao, L. H. *Inorg. Chem.* **2004**, *43*, 1799-1806.
- [44]. Icsel, C.; Yilmaz, V. T.; Ari, F.; Ulukaya, E.; Harrison, W. T. A. *Eur. J. Med. Chem.* **2013**, *60*, 386-394.
- [45]. Yeung, A. S.; Frank, C. W.; Singer, R. E. *Polymer* **1990**, *31*, 1092-1099.
- [46]. Wang, Y.; Chen, H.; Wu, H.; Li, X.; Weng, Y. *J. Am. Chem. Soc.* **2009**, *131*, 10711-10718.
- [47]. Xu, Z.; Singh, N. J.; Lim, J.; Pan, J.; Kim, H. N.; Park, S.; Kim, K. S.; Yoon, J. *J. Am. Chem. Soc.* **2009**, *131*, 15528-15533.
- [48]. Satyanarayana, S.; Dabrowiak, J. C.; Chaires, J. B. *Biochemistry* **1992**, *31*, 9319-9324.